Engineering 3 (2017) 653–662

Contents lists available at ScienceDirect

Engineering

journal homepage: www.elsevier.com/locate/eng

Research
Additive Manufacturing—Review

A Review on the 3D Printing of Functional Structures for Medical Phantoms and Regenerated Tissue and Organ Applications

Kan Wang [c], Chia-Che Ho [c], Chuck Zhang [a,c,*], Ben Wang [a,b,c]

[a] H. Milton Stewart School of Industrial and Systems Engineering, Georgia Institute of Technology, Atlanta, GA 30332, USA
[b] School of Materials Science and Engineering, Georgia Institute of Technology, Atlanta, GA 30332, USA
[c] Georgia Tech Manufacturing Institute, Georgia Institute of Technology, Atlanta, GA 30332, USA

ARTICLE INFO

Article history:
Received 6 June 2017
Revised 7 August 2017
Accepted 17 August 2017
Available online 31 October 2017

Keywords:
3D printing
3D bioprinting
Medical phantom
Regenerated tissue/organ
Scaffold

ABSTRACT

Medical models, or "phantoms," have been widely used for medical training and for doctor-patient interactions. They are increasingly used for surgical planning, medical computational models, algorithm verification and validation, and medical devices development. Such new applications demand high-fidelity, patient-specific, tissue-mimicking medical phantoms that can not only closely emulate the geometric structures of human organs, but also possess the properties and functions of the organ structure. With the rapid advancement of three-dimensional (3D) printing and 3D bioprinting technologies, many researchers have explored the use of these additive manufacturing techniques to fabricate functional medical phantoms for various applications. This paper reviews the applications of these 3D printing and 3D bioprinting technologies for the fabrication of functional medical phantoms and bio-structures. This review specifically discusses the state of the art along with new developments and trends in 3D printed functional medical phantoms (i.e., tissue-mimicking medical phantoms, radiologically relevant medical phantoms, and physiological medical phantoms) and 3D bio-printed structures (i.e., hybrid scaffolding materials, convertible scaffolds, and integrated sensors) for regenerated tissues and organs.

1. Introduction

Since its invention in the 1980s, techniques in three-dimensional (3D) printing, which is more formally referred to as additive manufacturing (AM), have been developed, matured, and applied in various applications by a large number of researchers and industrial companies worldwide. In its early years, 3D printing was primarily a rapid prototyping technique; today, it is revolutionizing manufacturing and many other industries with new processes, materials, and applications. In addition to plastic prototypes, complex engine components, houses, food, and even human organs can now be 3D printed. The 3D printing industry is experiencing rapid growth: Worldwide revenues of the industry grew by 17.4% in 2016 and are worth over $6 billion [1].

One major market for 3D printing is the medical field. For this important application area, 3D printing has provided effective solutions and shown great potential for personalized medicine and care. Current widely practiced medical uses of 3D printing include custom-made dentures, hearing aid shells, surgical and medical models, orthotic and prosthetic components, and artificial hip and knee implants [2–7]. One unique use of 3D printing technology is for the fabrication of "phantoms," or mock-ups of body parts, to allow doctors or surgeons to visualize body parts when preparing, planning, or optimizing complex medical operations or procedures [5,6]. Such phantoms can also be effective tools for surgical training and patient education purposes.

Since the early 2000s, 3D bioprinting technology has been developed and investigated by a number of research groups and biotech companies [8]. 3D bioprinting involves depositing layers of living cells onto gel media to build up 3D bio-functional structures. The

* Corresponding author.
E-mail address: chuck.zhang@gatech.edu

http://dx.doi.org/10.1016/J.ENG.2017.05.013

ultimate goal is to use the 3D printing technology for tissue engineering (TE) applications in order to build organs and body parts [9,10].

With the rapid advancement of 3D printing and 3D bioprinting technologies, a huge body of research and practical applications exists for these technologies. This paper reviews the applications of 3D printing and 3D bioprinting technologies, with a focus on fabrication of functional materials and structures for medical applications. This review specifically discusses the state of the art and trends for 3D-printed functional structures and bio-structures for medical phantoms and for regenerated tissue and organ applications.

2. 3D printing-enabled medical phantoms and structures

2.1. Need for physical medical phantoms

Medical imaging technologies have advanced dramatically in the past decade. With the evolution of imaging techniques such as multi-detector computed tomography (MD-CT) and magnetic resonance imaging (MRI), radiological diagnosis has become less invasive and more informative [11,12]. High-resolution 3D image data can be acquired in a short time. Image processing plays an increasingly important role in presenting human organs and structures with high fidelity and providing indispensable support in the diagnosis and treatment of many diseases and medical conditions [13–16]. Today's image-guided surgeries illustrate how radiologists have been integrated into therapeutic teams together with other surgical specialists. 3D visualization, multi-planar reformation, and image navigation help radiology to be pivotal in many clinical disciplines [17]. However, there is an unmet need to render digital imaging and communications in medicine (DICOM) images. Digital models are limited by the use of flat screens for the visualization of 3D imaging data. In addition to surgical planning applications, tangible medical phantoms are very useful for medical computational models validation, as well as for medical training and patient education. Therefore, there is a great need for high-fidelity physical medical phantoms for clinical practice and educational purposes.

2.2. Fabrication of medical phantoms

Physical medical phantoms have traditionally been produced by means of conventional manufacturing processes such as casting and molding. Such fabrication processes involve time-consuming and often expensive tooling preparation steps. In addition, it is not economical to fabricate individual, patient-specific medical phantoms due to the high tooling cost. Therefore, most of these phantoms are mass-produced, population-averaged, idealized models for general planning and educational purposes.

2.2.1. Tissue-mimicking medical phantoms

In medical imaging, phantoms are commonly used for developing and characterizing imaging systems or algorithms, as they provide imaging specimens with known geometric and material compositions. Tissue-mimicking medical phantoms can imitate the properties of biological tissue, and can therefore provide a more clinically realistic imaging environment [18]. In the past, casting or injecting molding processes have been used to fabricate tissue-mimicking medical phantoms. Applications of such phantoms can be found in the development and validation of medical imaging modalities such as ultrasound [19,20], MRI [21–24], computed tomography (CT) [25], and others [26]. With the increasing needs of biomedical research, other applications of tissue-mimicking medical phantoms, such as simulation of the electromagnetic properties of tissues [27], mechanical properties mimicking [28], and focused ultrasound ablation [29], have also been demonstrated. In those applications, phantoms were fabricated as population-averaged, idealized models, and the individual differences among patients were overlooked.

2.2.2. 3D printing of medical phantoms

3D printing technologies overcome the drawback of traditional manufacturing processes and are an effective tool for rapidly producing patient-specific, high-fidelity, medical phantoms at low cost, as the need for tooling is eliminated. 3D-printed medical models and phantoms fabricated from CT, MRI, or echocardiography data provide the advantage of tactile feedback, direct manipulation, and comprehensive understanding of a patient's anatomy and underlying pathologies. In many cases, 3D-printed medical phantoms can assist and facilitate surgeries and shorten the cycle times of medical procedures [30–33]. For example, an orthopedic surgery trainee used CT scan images to create printable copies of a patient's bones. He then had them printed and used these custom models to plan the patient's surgery [34]. 3D models have also been used for surgical planning by neurosurgeons [4,6]. Such 3D-printed neuroanatomical models can provide physical representations of some of the most complicated structures in the human body. These detailed high-fidelity phantoms can help neurosurgeons discover and visualize the intricate, sometimes obscured relationships between cranial nerves, vessels, cerebral structures, and skull architecture that are difficult to interpret based solely on two dimensional (2D) radiographic images [35]. This can reduce errors and avoid potentially devastating consequences in surgery.

2.3. Recent progress and future trends in functional medical phantoms

2.3.1. 3D printing of tissue-mimicking medical phantoms

Recent advances in computer-aided design (CAD), medical imaging, and 3D printing technologies have provided a rapid and cost-efficient method of generating patient-specific, tissue-mimicking medical phantoms from computational models that are reconstructed from the CT or MRI results of individuals [36]. Those patient-specific phantoms have unparalleled advantages in many biomedical applications, such as computational model validation, medical device testing, surgery planning, medical education, and doctor-patient interaction. Biglino et al. [37] demonstrated the fabrication of compliant arterial phantoms with PolyJet™ technology by Stratasys Ltd. (Eden Prairie, MN), an AM technique that deposits a liquid photopolymer layer by layer through orifice jetting and then solidifies it by UV exposure. A rubber-like material named TangoPlus was used in this study for its mechanical properties, which are close to those of real tissue. Cloonan et al. [36] conducted a comparative study on the use of common tissue-mimicking materials and 3D printing materials, including TangoPlus, for abdominal aortic aneurysm phantoms. Their results suggested that TangoPlus was a suitable material for modeling arteries in terms of dispensability, and that its uniaxial tensile properties outperformed those of poly(dimethylsiloxane) (PDMS) SYLGARD elastomers, which are commonly used in the investment casting process.

2.3.2. Radiologically relevant medical phantoms

3D printing technologies have been used to fabricate radiology-realistic phantoms that have regions with different attenuations [38]. In this study, the multi-material PolyJet™ printing technique from Stratasys Ltd. was used to construct liver and brain phantoms with realistic pathologies, anatomic structures, and heterogeneous backgrounds. The liver and head CT images of patients were segmented into tissue, vessels, liver lesions, white and gray matter, and cerebrospinal fluid. Printing materials that had different CT numbers were assigned to these objects after test scans. Finally, 3D-printed

phantoms were scanned on a CT scanner and the images were evaluated. It was found that for the liver, the patient and phantom images had a similar texture. CT images of the brain phantom showed that the CT number differences of objects of interest were similar to those in the patient images. These phantoms have heterogeneous backgrounds and realistic pathology that is similar to that of the real tissue, and could potentially be used for image-quality assessment, radiation dose reduction, and other research and educational activities.

2.3.3. Physiological medical phantoms

Patient-specific and tissue-mimicking medical phantoms contain individual information, and hold great potential for many biomedical applications and clinical benefits, such as computational model validation, medical device testing, surgery planning, medical education, and doctor-patient interaction. As described previously, the 3D printing technology has proven to be an effective manufacturing method of fabricating such phantoms. However, the existing technologies are still inadequate in fully mimicking human organs and tissues. For example, many human organ structures, such as heart valves, have anisotropic mechanical properties due to directional tissue structures; however, the regular 3D-printed phantoms do not possess the same special anisotropic mechanical properties. Therefore, most 3D-printed medical phantoms, even those with patient-specific and tissue-mimicking features, are only anatomically—not physiologically—close to human organ structures.

Most medical phantoms are made using polymeric materials. Although the uniaxial tensile properties of phantom materials can be close to those of soft tissues within the small strain (< 3%) range, the creep tendency, which is an inherent characteristic of polymers, makes them behave quite differently than soft tissues under larger deformation. For tissue-mimicking medical phantoms, the strain range of interest is normally the working strain range of the tissue. As shown in Fig. 1 [39], soft tissues typically exhibit a strain-stiffening behavior initially, which is represented by a convex stress-strain curve in the beginning. As the strain increases, the curve changes from convex to concave, which indicates yielding of the material [40]. In contrast, polymeric materials typically have a concave stress-strain curve at the beginning, indicating strain softening. Even though the initial Young's modulus of a polymeric phantom can be designed to match the Young's modulus of real tissues, the mechanical behavior of the phantom will deviate from that of real tissue at higher strain levels.

Wang et al. [39,41] demonstrated an integrated metamaterial design and multi-material 3D printing approach to fabricate medical phantoms that possess the properties of real soft tissues. Metamaterials are artificially structured materials for achieving and manipulating certain physical properties and/or phenomena. The properties of metamaterials are derived both from the inherent properties of their constituent materials and from the geometrical arrangement of those materials [42,43]. In the context of tissue-mimicking medical phantoms, the key value of the "metamaterial" concept is the idea of constructing artificial models of tissue with heterogeneous microstructures that, although difficult to construct by conventional means, can easily be rendered using 3D printing. With multi-material 3D printing technology, the feasibility of designing the mechanical properties of metamaterials has been proven [39,41]. These studies investigated the feasibility of mimicking the strain-stiffening behavior of soft tissues using dual-material 3D-printed metamaterials with microstructured reinforcement embedded in a soft polymeric matrix. Three types of metamaterials were designed and tested: sinusoidal wave, double helix, and interlocking chain designs (Fig. 2) [39]. Even though the two base materials were strain-softening polymers, both finite element analysis and uniaxial tension tests indicated that two of the dual-material designs were able to exhibit strain-stiffening effects as a metamaterial. The effects of the design parameters on the mechanical behavior of the metamaterials were also demonstrated (Fig. 3) [39]. The results suggested that the fabrication of patient-specific tissue-mimicking medical phantoms with both geometrical and mechanical accuracies is possible with dual-material 3D-printed metamaterials.

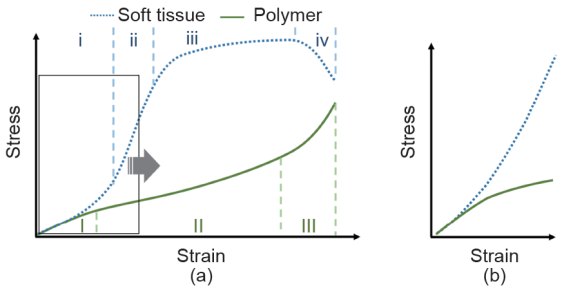

Fig. 1. Comparison of the mechanical behaviors of soft tissue and polymer. (a) Typical stress-strain curves of soft tissue (dotted line) and polymer (solid line). Soft tissue: i—toe region, ii—elastic region, iii—plastic region, iv—failure region; polymer: I—primary creep, II—secondary creep, III—tertiary creep. (b) Magnified view of the curves in the strain range of interest for most tissue-mimicking medical phantoms [39].

2.3.4. Applications of physiological medical phantoms

In addition to the conventional applications of medical phantoms, physiological medical phantoms are finding new and unique uses in medical fields. In a recent study, Qian et al. [44] demonstrated the efficacy of using physiological patient-specific phantoms to plan the trans-catheter aortic valve replacement (TAVR) procedure. (TAVR is a less invasive treatment option for severe aorta stenosis patients who are at high surgical risk.) In order to achieve optimal clinical outcomes, an individualized assessment of the interactions between the native aortic tissue, the prosthesis, and the blood flow is critical. This study aimed to develop a procedure simulation platform for *in vitro* TAVR implantation using 3D-printed physiological

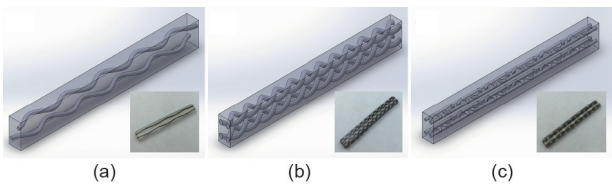

Fig. 2. CAD models and printed samples of three metamaterials: (a) sinusoidal wave design, (b) double helix design, and (c) interlocking chain design [39].

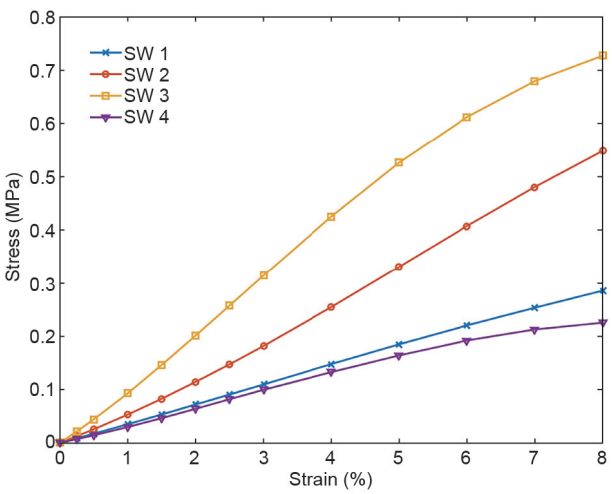

Fig. 3. Stress-strain curves of the four variants of the sinusoidal wave (SW) design [39].

tissue-mimicking medical phantoms. The researchers also investigated the feasibility of applying this platform to quantitatively predict the occurrence, severity, and location of any post-TAVR paravalvular leaks (PVLs), which are an independent risk factor for increased short- and long-term mortality. In this study, physiological aortic heart valves based on real patient data (i.e., CT images) were fabricated using the integrated metamaterial design and multimaterial 3D printing approach described in Subsection 2.3.3 [39,41]. Fig. 4 [44] shows the CT images of a patient's aortic root, the 3D computational model, and the 3D-printed physiological phantom. The test and analysis outcomes using the 3D-printed physiological valves indicated the locations of the final PVL in the 12 patients who had a certain degree of PVL after TAVR, as well as the sites of the maximum annular bulge index, a predictor for PVL occurrence (Fig. 5) [44]. The predictions of the location of the dominant PVL from 3D-printed valves matched well with the actual PVL occurrence in the patients, with an accuracy of 75% [44]. In this proof-of-concept study, the researchers demonstrated the feasibility of using 3D-printed physiological patient-specific phantoms to quantitatively assess post-TAVR aortic root strain *in vitro*.

3. Additive manufacturing of regenerated tissues and organs

Owing to the increasing demand for tissue and organ transplantation, and the deficiency of tissue and organ donors, numerous efforts have been made in the field of TE to develop biological substitutes for native human tissues and organs [45–47]. For TE purposes, biodegradable scaffolds with high porosity and interconnectivity can be employed to provide shape, mechanical support, and microarchitecture for cellular growth and reorganization in order to improve and accelerate the healing and repairing process [46,48]. In this regard, the design of TE scaffolds plays a dominant role in the successful rate of treatments. Different strategies for creating 3D scaffolds have been proposed and investigated, such as freeze-drying [49,50], gas foaming [51], phase separation [52], porogen leaching [53], and electrospinning [54,55]. However, precise control of the porosity and internal microstructure of the scaffold manufactured by these routes in order to manipulate oxygen, nutrients, and soluble biomolecules for promoting cell growth and differentiation is still challenging. In addition, directing different types of cell growth in TE scaffolds in order to form functional tissues that are organized at a level of complexity is a major engineering design obstacle [56]. Although a few exciting clinical results have been reported on autologous cell-loaded scaffolds with uncomplicated structural design being capable of guiding the regeneration of multifunctional tissues and organs [45,57,58], advanced strategies for manufacturing acellular or cell-laden bioscaffolds with higher levels of complexity are still in progress [46,59–62]. Advances in AM techniques have been a recent breakthrough in TE and regenerative medicine. A growing amount of interest has focused on manufacturing complex and functional 3D bioscaffolds with specific biomaterials and cells in order to provide a microenvironmental and biological componential similarity to the native tissue for TE application. To date, several types of bioprinting systems that are capable of constructing either acellular or cell-laden hydrogel scaffolds have been described in the literature. The three most important and well-established techniques for bioprinting are laser-induced forward transfer (LIFT), inkjet bioprinting, and robotic dispensing.

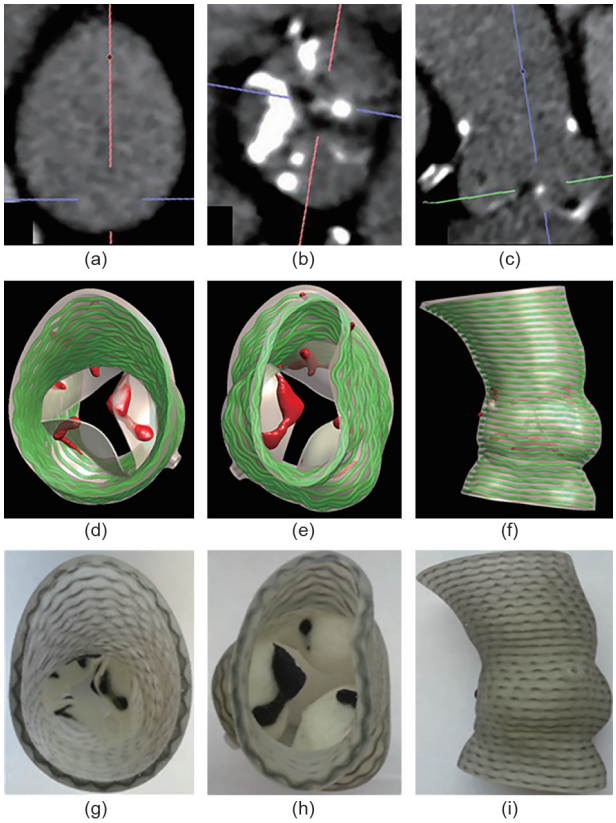

Fig. 4. An example of CT images of the aortic root, the 3D computational model, and the 3D-printed physiological phantom. (a), (b), and (c) show the CT cross-sectional views at the ascending aorta and the valves, and the longitudinal view, respectively. (d), (e), and (f) show the 3D computational model viewed from the ascending aorta, the left ventricular outflow tract (LVOT), and the side, respectively. The aortic wall and leaflets are depicted semi-transparently, the calcifications are drawn in red, and the embedded fibers are drawn in green. (g), (h), and (i) show the 3D-printed physiological phantom. The calcifications and the fibers are printed with black materials for better illustration [44].

3.1. Bioprinting strategies

LIFT is a technique that can deposit cells onto a receiving substrate. In general, a laser pulsed beam is applied on a donor slide or ribbon containing source inks (i.e., hydrogels and cells), followed by the evaporation of the inks; this results in a high-pressure bubble jetting toward the receiving substrate, which is placed underneath the donor slide. By controlling the movement of the donor slide or the substrate, a deposited 2D pattern can be built up to form 3D constructs in a layer-by-layer fusion [49,63–65]. For example, Michael's group [66] utilized this technique to create a fully cellularized skin substrate that mimicked the microenvironment of the native skin by printing fibroblasts and keratinocytes on top of an acellular dermal substitute (Matriderm®). The results of *in vivo* experiments demonstrated that the printed cells survived well, and neovascularization could be observed in the skin construct, implying that laser printing may be an adequate strategy for the creation of 3D tissues. Heterogeneous constructs with multiple cell types can also be built up by inkjet printing. Xu et al. [67] fabricated a pie-shaped 3D construct consisting of stem cells, smooth muscle cells, and endothelial cells using a thermal inkjet printer. In contrast to the common method of inkjet bioprinting, which usually ejects inks onto solid substrates to obtain a 3D construct [68–70], the cells were combined with calcium chloride ($CaCl_2$) to form bioinks and the inks were ejected into an alginate-collagen solution. The portion of the polymer solution surface that was impacted by the ink droplets was instantaneously solidified due to the formation of the egg-box structure of the Ca^{2+}-alginate complexes. The results of the *in vitro* experiments indicated that the printed cells were able to survive, proliferate, and maintain cellular function in the 3D construct. More importantly, the stem cells and endothelial cells were capable of differentiating into bone and blood vessels after respective implantation into mice

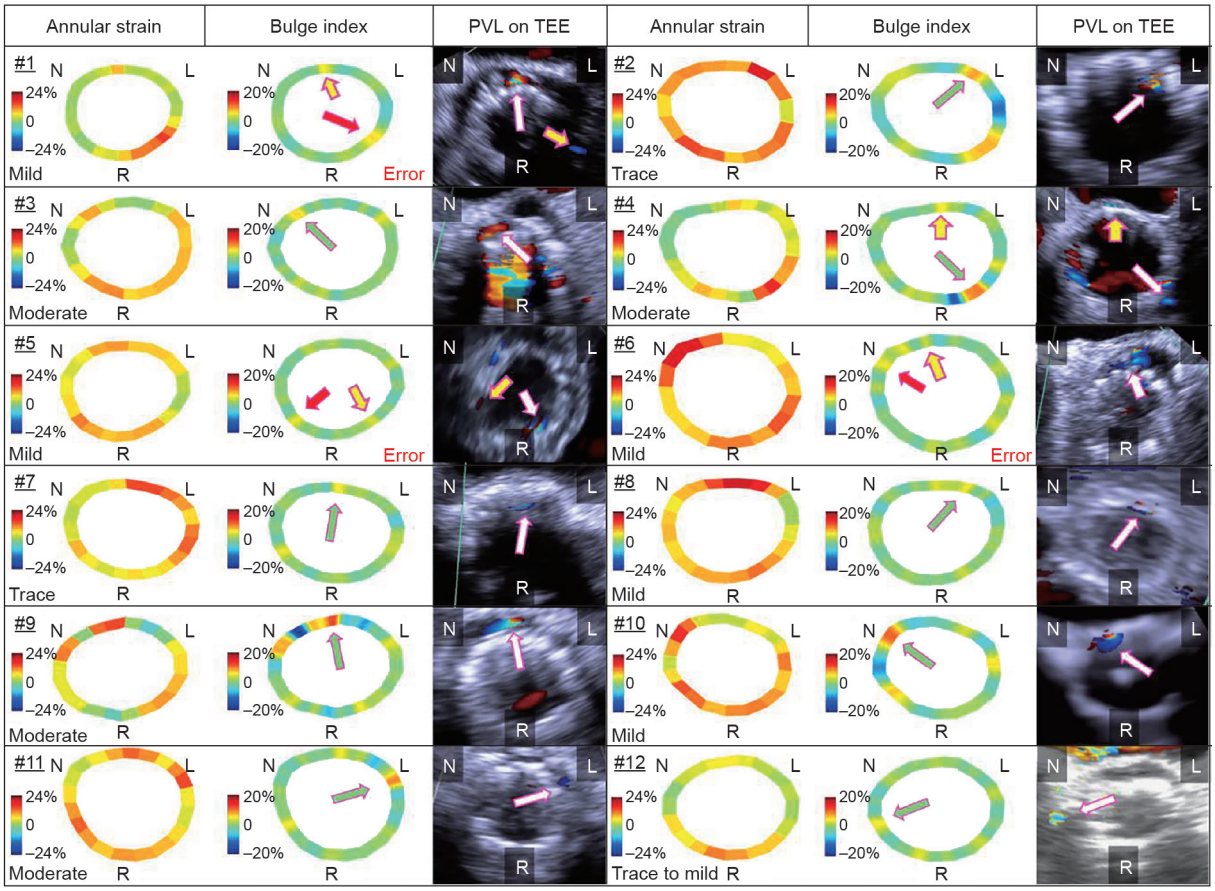

Fig. 5. Prediction of the PVL locations in 12 patients who had a certain degree of post-TAVR PVL. In the bulge index images, green arrows indicate correct prediction of the dominant PVL sites; red arrows indicate that the maximum bulge index did not predict the dominant PVL site; yellow arrows indicate that a submaximal high bulge index corresponded to the dominant PVL site. In the transesophageal echocardiography (TEE) images, white arrows indicate the dominant PVL sites, and yellow arrows indicate the minor PVL sites [44].

for six weeks.

In contrast to the LIFT technique, the major disadvantage of inkjet bioprinting is that the viability of the printed cells can be remarkably diminished by the critical shear stress that is generated when the bioinks pass through the nozzle and deposit on the substrates [59,66]. In addition, cell sedimentation occurs due to cell aggregation during printing, and results in nozzle clogging and inhomogeneous cell distribution in the constructs [65,68,71]. Although both techniques possess the ability to precisely create 3D constructs that are composed of multiple cell types on demand, these printing strategies usually produce small-scale constructs, which is an obstacle for practical use in clinical applications [63,71]. Inspired by outstanding performances in the creation of 3D cell constructs using LIFT and inkjet bioprinting, a large number of studies have focused on the development of a robotic dispensing system for bioprinting (i.e., extrusion-based bioprinting, or EBB) owing to its easy-to-use nature and good compatibility with different bioinks [72]. EBB allows the manufacture of 3D constructs on a millimeter scale by the pneumatically or mechanically driven dispensation of biopolymers or synthetic biopolymers in a layer-by-layer fashion [72–75]. Mini-tissues (i.e., spheroids and organoids) composed of multiple cellular types can serve as the building blocks for large tissues and organs that are printed using EBB [76,77]. However, several technical gaps need to be addressed in order to improve the structural and componential freedom of these 3D constructs. The primary limitation is that only one bioink can be used for each printing process; this raises the difficulty of the construction of 3D architectures with high levels of complexity. Increasing the number of reservoirs on the printer could be done to achieve printe with multiple bioinks. Of course, the printing speed of the constructs was reduced as a result, since more steps were included in the printing process [72,73,78]. A pneumatic-driven multi-material bioprinter was recently developed by Liu et al. [72]. The printer they developed has the ability to eject seven types of bioink, both individually and simultaneously, by routing different reservoirs into a single print head. It is interesting to note that the novel design of the print head allows different bioinks to mix at a controllable feeding rate before extrusion in order to achieve gradient printing in a single strut.

3.2. Recent progress and future trends

Recent advances in AM technologies have enabled several new TE pathways. In particular, the following three strategies are gaining momentum now that new AM technologies have become available: ① the development of hybrid scaffolding materials to achieve tunable properties of scaffolds; ② the design of special microstructures to achieve convertibility of scaffolds; and ③ the integration of sensors to achieve built-in process-monitoring capability. The details of and future predictions for each strategy are discussed below.

3.2.1. Hybrid scaffolding materials

Biopolymers, such as polycaprolactone (PCL), polylactic acid (PLA), and poly(lactic-*co*-glycolic acid) (PLGA), are the most commonly used base materials for scaffolding. In most cases, they are not a perfect fit for TE due to their relatively weak mechanical properties, poor cell adhesion, or near-inert bioactivity. By

blending additives into the biopolymers, those disadvantages can be mitigated. Many of these additives are bioceramics in powder form. For example, α-tricalcium phosphate (α-TCP) has been added to PCL [53] to improve mechanical properties, cell seeding, and proliferation. β-tricalcium phosphate (β-TCP) has been used as an additive in PCL [79,80], PLA [81], and PLGA [82] to enhance mechanical and hydrophilic properties. In bone TE, it can also improve the biocompatibility and osteoconductivity in the physiological environment due to its bioresorbability and chemical similarity to the mineral phase of bone. It is clinically proven that β-TCP promotes osteogenic and odontogenic differentiation in various types of cells. Hydroxyapatite (HA) is an even more common additive for bone TE because its chemical composition is similar to that of the inorganic part of native bones. It has been used in PCL [83–93], PLA [93–97], poly(*D*,*L*-lactic acid)-poly(ethylene glycol)-poly(*D*,*L*-lactic acid) (PELA) [98,99], PLGA [82], and poly-*D*,*L*-lactide (PDLLA) [100]. Biopolymers with HA additives have exhibited excellent chemical and biological affinity to bone tissues. Other additives used in scaffolding biopolymers include bioactive glass particles [101–103], collagen [104], calcium silicate [91,105], calcium phosphate [106,107], magnesium (Mg) [105,108], and alginates [104,109,110].

More recent studies have explored various nanomaterials as additives for biopolymers. These nanomaterials usually add new functions to the base material. For example, adding magnesia (MgO) [83] to PCL affects the modulation of signal transduction, energy metabolism, and cell proliferation, which promotes new bone formation. Adding magnetic nanoparticles (Fe_3O_4 or γ-Fe_2O_3) [89,111] to PCL grants the scaffold the ability of magnetic heating, which significantly stimulates proliferation. Other nanomaterials, such as nanoclay [112], single-wall carbon nanotubes (SWCNTs) [113,114], multi-wall carbon nanotubes (MWCNTs) [85,114–119], graphene [117], and graphene oxide (GO) have been added to PCL or PLA to modify the mechanical, electrical, and thermal properties of the base biopolymer.

Current manufacturing methods of scaffolds with hybrid materials all start with premixing the biopolymer and the additives. The prepared mixture is then used to build the scaffold, by either 3D printing or any top-down method. This procedure ensures the homogeneous distribution of additives in the biopolymer matrix. However, the disadvantage is obvious: The composition of the hybrid material is fixed. If the goal is to regenerate a complex, multi-cell-type organ, different compositions are required at different locations on the scaffold. Using the more recent AM technologies, it is possible to mix the biopolymer and additives *in situ* during scaffold printing. Fig. 6 shows the conceptual setup for multi-material 3D bioprinting. In this way, future hybrid scaffolds will have tunable properties and extra designed functions, which will benefit the differentiation and growth of multiple cell types to form complicated biological structures.

3D bioprinting can also be combined with direct-write technologies. Direct-write technologies are conventionally used in the printed electronics industry as an alternative to lithography or screen printing. By integrating direct-write technologies, the 3D bioprinting process can perform selective surface modification during scaffolding. Fig. 7 demonstrates a conceptual setup of 3D bioprinting with *in situ* growth factor grafting using extrusion and aerosol jet printing technologies.

Fig. 8 compares two strategies for fabricating scaffolds with multiple growth factors. Although the pre-mix method requires more material preparation steps, its printing process is relatively straightforward with multi-head 3D printers. The two growth factors are also less likely to cross-contaminate during printing. The *in situ* grafting method does not require a material preparation step, but requires integration of 3D printing and layer coating for the building of each layer. Depending on the coating technology, there is a risk of cross-contamination between two growth factors. However, the coating step is independent of the scaffold-printing step, which enables a higher degree of design freedom and more detailed coating patterns.

3.2.2. Convertible scaffold

Bioprinting technologies provide precise control over the initial cell distribution in the printed construct. However, once the cells start to grow in the bioreactor and regenerate into the tissue via the self-assembly process, no control method is currently available to ensure an optimal microenvironment throughout the scaffold at all times. In other words, when bioprinting TE scenarios at present, too much of the cell growth process is uncontrolled. Cell growth is a spatiotemporal process with intrinsically high variability in quality, quantity, yield, and other metrics. Although the behavior of each individual cell is not readily predictable, the growth of a cell culture within a large population is largely controllable with environmental factors, including local cell density [75,81] and ion-exchange rate [108,111]. In a cell culture process without a scaffold, certain agitation or perfusion mechanisms are typically used to ensure near-uniform local cell distribution and to promote nutrient, growth factor, and waste exchange. A scaffold will hinder the nutrient, growth factor, and waste exchange of cells. Studies have indicated that cell growth on a scaffold is not optimal in terms of growth rate [102,108] and cell viability [92] once the cell density reaches a certain point.

Using 3D-printed auxetic metamaterials as scaffolds may provide a solution in the near future. Auxetic metamaterials [119,120] are materials with repeated microstructures that exhibit a negative Poisson's ratio in the macroscale, which allows the volume to change in a unique way for the overall construct. Advances in 3D printing have enabled and accelerated novel designs and applications of auxetic metamaterials [93,104,121]. With auxetic metamaterials as

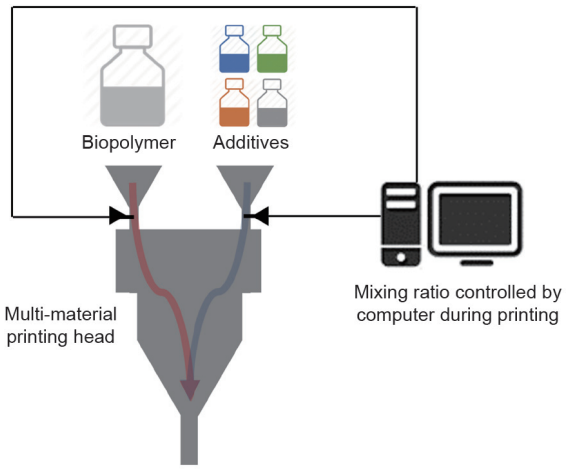

Fig. 6. A conceptual setup for multi-material 3D bioprinting.

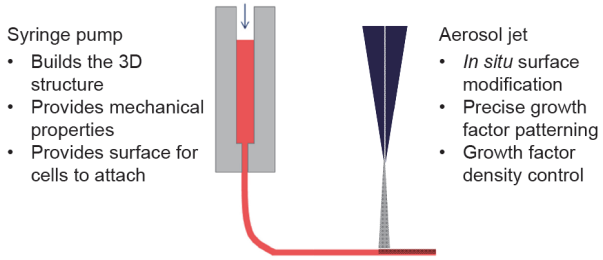

Fig. 7. A conceptual setup for *in situ* surface modification.

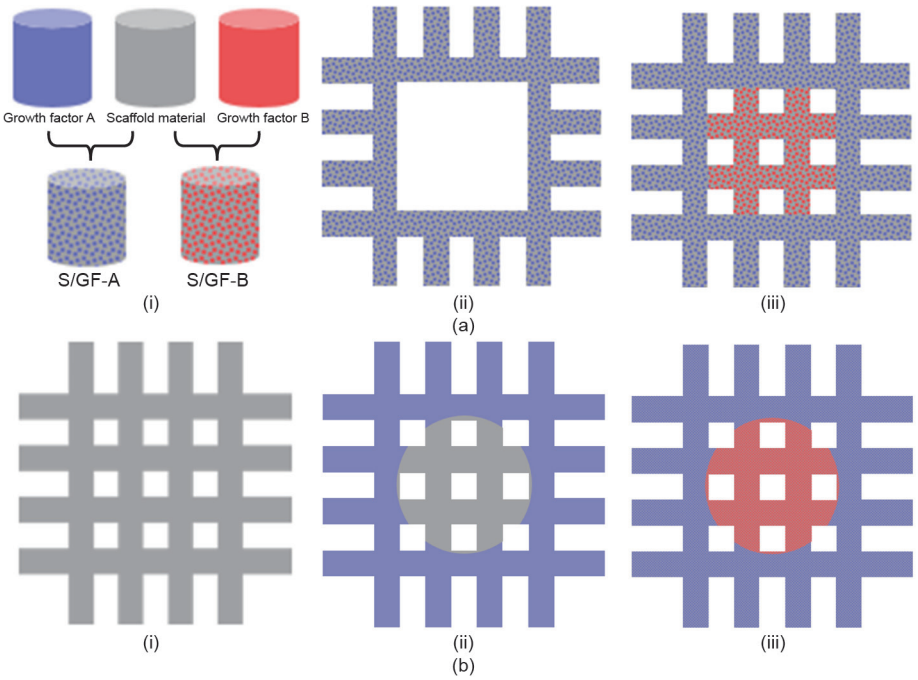

Fig. 8. Comparison of pre-mix method and *in situ* grafting method for fabricating scaffolds with multiple growth factors. (a) Pre-mix method: (i) mixing scaffold material with growth factors, (ii) printing scaffold material/growth factor A (S/GF-A) as the scaffold at region A, (iii) printing scaffold material/growth factor B (S/GF-B) as the scaffold at region B; (b) *in situ* grafting method: (i) printing the scaffold with pure scaffold material, (ii) coating region A with growth factor A, (iii) coating region B with growth factor B.

scaffolds, the ability to change volume provides an effective way to control the local cell density. In addition, the change of porosity that comes with the volume change implies that the culture medium flows in and out the scaffold, replenishing nutrients for the internal cells and taking away the waste. Fig. 9 shows a double-arrow type of auxetic metamaterial.

3.2.3. Integrated sensors

Direct-write technologies are a class of AM methods that can fabricate electronic circuits without masking [122]. These relatively new technologies include inkjet printing, aerosol jet printing, syringe dispensing, laser-assisted chemical vapor deposition, laser particle guidance, matrix-assisted pulsed-laser evaporation, and focused ion beam. Direct-write processes are fast and flexible, and have a high tolerance for errors. Some direct-write technologies, such as aerosol jet printing, do not require the substrate to be planar. This provides opportunities to integrate sensors into bio-printed scaffolds.

In most cases, direct-write technologies are used to create conductive patterns. Metallic nanoparticle pastes or dispersions are used as inks in such cases. These include silver, gold, and copper nanoparticles as the three most common materials. Carbon-based inks are also a popular family that is recently adopted in many direct-write technologies and their applications. This includes carbon nanotubes, graphite, graphene, decorated carbon nanotubes, and their mixtures. Some researchers have reported that mixtures of inks with carbon-based nanomaterials and metallic nanoparticles have potential in stretchable electronics printing [122].

With more and more complex functions and designs of printed electronics, there are demands for more types of specialized inks, other than conductive inks. For example, boron nitride nanotubes (BNNTs) can be dispersed into certain solvents to create a piezoelectric ink. There are many applications for a thin layer of patterned dielectric material. Both inorganic and polymeric dielectric inks have been developed, and semiconductor nanoparticle inks and polymer semiconductor inks are on the market. Some recent research is developing biological inks that can be printed by aerosol jet printing.

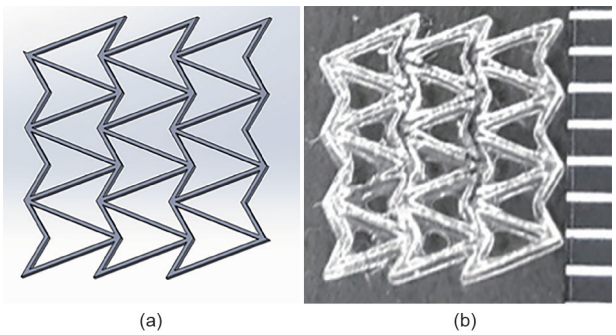

Fig. 9. A double arrowhead auxetic design. (a) Computer-aided design; (b) microscopic picture of a scaffold printed by GeSiM™ bioplotter (distance between marks is 1 mm).

Fig. 10 summarizes the inks that are most commonly used by various direct-write technologies.

On the manufacturing level, the use of direct-write technologies to introduce a sensing capability to smart scaffolds is encountering a set of challenges that include scalability, yield, toxicity, environmental impact, and supply-chain design. Different direct-write technologies are at different manufacturing readiness levels (MRLs). In general, this strategy is still in the proof-of-concept stage. The overall outlook for the smart scaffold field suggests that interest and attention in integrating sensors into TE has increased significantly during the last decade. It is reasonable to believe that more and more smart scaffold designs will include certain kinds of direct-write technologies in the near future.

4. Conclusions

This paper provides a review of various applications of AM techniques in the construction of functional medical phantoms and in the fabrication of regenerated tissues and organs. Existing work, results, recent progress, and future trends were discussed. In the field of functional medical phantoms, recent work in the 3D printing of

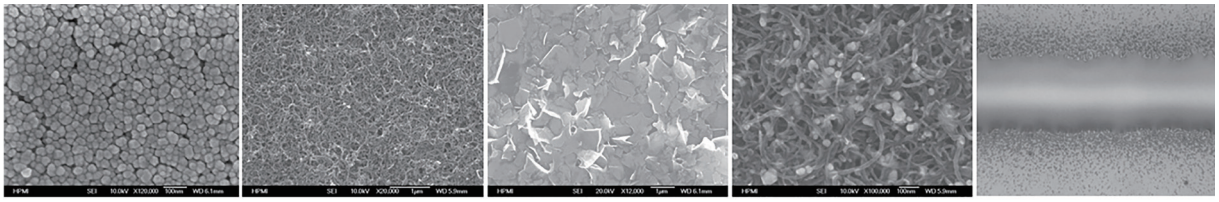

(a) (b) (c) (d) (e)

Fig. 10. Typical inks used in various direct-write technologies, including (a) metal nanoparticles, (b) carbon nanotubes, (c) graphite, (d) carbon nanotubes/silver nanoparticles, and (e) polyimide.

tissue-mimicking medical phantoms, radiologically relevant medical phantoms, and physiological medical phantoms has been presented. A detailed discussion was provided on the design and fabrication of physiological medical phantoms. A case for the application of such physiological medical phantoms to surgical planning for the TAVR procedure was presented. In the field of regenerated tissues and organs, existing work and results for 3D bioprinting of these functional bio-structures were reviewed. Recent work in and future trends for the application of emerging AM technologies in this field were presented, including hybrid scaffolding materials, convertible scaffolds, and integrated sensors. From this review of previous and new research work and results, it can be seen that emerging AM technologies have great potential to produce effective functional structures for the advancement of medical care and the realization of personalized medicine.

Compliance with ethics guidelines

Kan Wang, Chia-Che Ho, Chuck Zhang, and Ben Wang declare that they have no conflict of interest or financial conflicts to disclose.

References

[1] Kianian B. Wohlers report 2017—3D printing and additive manufacturing state of the industry—Annual worldwide progress report. Fort Collins: Wohlers Associates, Inc.; 2017.

[2] Wu J, Li Y, Zhang Y. Use of intraoral scanning and 3-dimensional printing in the fabrication of a removable partial denture for a patient with limited mouth opening. J Am Dent Assoc 2017;148(5):338–41.

[3] Banks J. Adding value in additive manufacturing: Researchers in the United Kingdom and Europe look to 3D printing for customization. IEEE Pulse 2013;4(6):22–6.

[4] Klein GT, Lu Y, Wang MY. 3D printing and neurosurgery—Ready for prime time? World Neurosurg 2013;80(3–4):233–5.

[5] Gross BC, Erkal JL, Lockwood SY, Chen C, Spence DM. Evaluation of 3D printing and its potential impact on biotechnology and the chemical sciences. Anal Chem 2014;86(7):3240–53.

[6] National Institutes of Health. NIH 3D print exchange [Internet]. [cited 2014 Jul 9]. Available from: http://3dprint.nih.gov.

[7] Zopf DA, Hollister SJ, Nelson ME, Ohye RG, Green GE. Bioresorbable airway splint created with a three-dimensional printer. N Engl J Med 2013; 368(21):2043–5.

[8] Peltola SM, Melchels FP, Grijpma DW, Kellomäki M. A review of rapid prototyping techniques for tissue engineering purposes. Ann Med 2008;40(4):268–80.

[9] Mironov V, Boland T, Trusk T, Forgacs G, Markwald RR. Organ printing: Computer-aided jet-based 3D tissue engineering. Trends Biotechnol 2003;21(4):157–61.

[10] Murphy SV, Atala A. 3D bioprinting of tissues and organs. Nat Biotechnol 2014;32(8):773–85.

[11] Kido T, Kurata A, Higashino H, Sugawara Y, Okayama H, Higaki J, et al. Cardiac imaging using 256-detector row four-dimensional CT: Preliminary clinical report. Radiat Med 2007;25(1):38–44.

[12] Meaney JF, Goyen M. Recent advances in contrast-enhanced magnetic resonance angiography. Eur Radiol 2007;17(Suppl 2):B2–6.

[13] Rengier F, Mehndiratta A, von Tengg-Kobligk H, Zechmann CM, Unterhinninghofen R, Kauczor HU, et al. 3D printing based on imaging data: Review of medical applications. Int J Comput Assist Radiol Surg 2010;5(4):335–41.

[14] Mitsouras D, Liacouras P, Imanzadeh A, Giannopoulos AA, Cai T, Kumamaru KK, et al. Medical 3D printing for the radiologist. Radiographics 2015;35(7):1965–88.

[15] Doi K. Diagnostic imaging over the last 50 years: Research and development in medical imaging science and technology. Phys Med Biol 2006;51(13):R5–27.

[16] Kirchgeorg MA, Prokop M. Increasing spiral CT benefits with postprocessing applications. Eur J Radiol 1998;28(1):39–54.

[17] Mahesh M. Search for isotropic resolution in CT from conventional through multiple-row detector. Radiographics 2002;22(4):949–62.

[18] Cook JR, Bouchard RR, Emelianov SY. Tissue-mimicking phantoms for photoacoustic and ultrasonic imaging. Biomed Opt Express 2011;2(11):3193–206.

[19] Madsen EL, Kelly-Fry E, Frank GR. Anthropomorphic phantoms for assessing systems used in ultrasound imaging of the compressed breast. Ultrasound Med Biol 1988;14(Suppl 1):183–201.

[20] Madsen EL, Zagzebski JA, Frank GR. An anthropomorphic ultrasound breast phantom containing intermediate-sized scatters. Ultrasound Med Biol 1982;8(4):381–92.

[21] Blechinger JC, Madsen EL, Frank GR. Tissue-mimicking gelatin-agar gels for use in magnetic resonance imaging phantoms. Med Phys 1988;15(4):629–36.

[22] Fong PM, Keil DC, Does MD, Gore JC. Polymer gels for magnetic resonance imaging of radiation dose distributions at normal room atmosphere. Phys Med Biol 2001;46(12):3105–13.

[23] Madsen EL, Fullerton GD. Prospective tissue-mimicking materials for use in NMR imaging phantoms. Magn Reson Imaging 1982;1(3):135–41.

[24] Surry KJ, Austin HJ, Fenster A, Peters TM. Poly(vinyl alcohol) cryogel phantoms for use in ultrasound and MR imaging. Phys Med Biol 2004;49(24):5529–46.

[25] Kruger RA, Kopecky KK, Aisen AM, Reinecke DR, Kruger GA, Kiser WL Jr. Thermoacoustic CT with radio waves: A medical imaging paradigm. Radiology 1999;211(1):275–8.

[26] D'Souza WD, Madsen EL, Unal O, Vigen KK, Frank GR, Thomadsen BR. Tissue mimicking materials for a multi-imaging modality prostate phantom. Med Phys 2001;28(4):688–700.

[27] Lazebnik M, Madsen EL, Frank GR, Hagness SC. Tissue-mimicking phantom materials for narrowband and ultrawideband microwave applications. Phys Med Biol 2005;50(18):4245–58.

[28] Wang RK, Ma Z, Kirkpatrick SJ. Tissue Doppler optical coherence elastography for real time strain rate and strain mapping of soft tissue. Appl Phys Lett 2006;89(14):144103.

[29] Sun MK, Shieh J, Lo CW, Chen CS, Chen BT, Huang CW, et al. Reusable tissue-mimicking hydrogel phantoms for focused ultrasound ablation. Ultrason Sonochem 2015;23:399–405.

[30] Schubert C, van Langeveld MC, Donoso LA. Innovations in 3D printing: A 3D overview from optics to organs. Br J Ophthalmol 2014;98(2):159–61.

[31] Lipson H. New world of 3D printing offers "completely new ways of thinking": Q&A with author, engineer, and 3D printing expert Hod Lipson. IEEE Pulse 2013;4(6):12–4.

[32] Hoy MB. 3D printing: Making things at the library. Med Ref Serv Q 2013; 32(1):94–9.

[33] Ionita CN, Mokin M, Varble N, Bednarek DR, Xiang J, Snyder KV, et al. Challenges and limitations of patient-specific vascular phantom fabrication using 3D PolyJet printing. Proc SPIE Int Soc Opt Eng 2014;9038:90380M.

[34] 3D printing bone on a budget [Internet]. New York: Shapeways, Inc.; c2008–2017 [updated 2011 Sep 14; cited 2017 Jun 6]. Available from: https://www.shapeways.com/blog/archives/995-3D-Printing-Bone-on-a-budget!.html.

[35] Ventola CL. Medical applications for 3D printing: Current and projected uses. P T 2014;39(10):704–11.

[36] Cloonan AJ, Shahmirzadi D, Li RX, Doyle BJ, Konofagou EE, McGloughlin TM. 3D-printed tissue-mimicking phantoms for medical imaging and computational validation applications. 3D Print Addit Manuf 2014;1(1):14–23.

[37] Biglino G, Verschueren P, Zegels R, Taylor AM, Schievano S. Rapid prototyping compliant arterial phantoms for *in vitro* studies and device testing. J Cardiovasc Magn Reson 2013;15:2.

[38] Leng S, Chen B, Vrieze T, Kuhlmann J, Yu L, Alexander A, et al. Construction of realistic phantoms from patient images and a commercial three-dimensional printer. J Med Imag 2016;3(3):033501.

[39] Wang K, Wu C, Qian Z, Zhang C, Wang B, Vannan MA. Dual-material 3D printed metamaterials with tunable mechanical properties for patient-specific tissue-mimicking phantoms. Addit Manuf 2016;12(Part A):31–7.

[40] Raghavan ML, Webster MW, Vorp DA. *Ex vivo* biomechanical behavior of abdominal aortic aneurysm: Assessment using a new mathematical model. Ann Biomed Eng 1996;24(5):573–82.

[41] Wang K, Zhao Y, Chang YH, Qian Z, Zhang C, Wang B, et al. Controlling the mechanical behavior of dual-material 3D printed meta-materials for patient-specific tissue-mimicking phantoms. Mater Des 2016;90:704–12.

[42] Center for Metamaterials and Integrated Plasmonics. Metamaterials [Internet]. [cited 2017 Jun 6]. Available from: http://metamaterials.duke.edu/research/

metamaterials.
[43] Lee JH, Singer JP, Thomas EL. Micro-/nanostructured mechanical metamaterials. Adv Mater 2012;24(36):4782–810.
[44] Qian Z, Wang K, Liu S, Zhou X, Rajagopal V, Meduri C, et al. Quantitative prediction of paravalvular leak in transcatheter aortic valve replacement based on tissue-mimicking 3D printing. JACC Cardiovasc Imag 2017;10(7):719–31.
[45] Atala A, Bauer SB, Soker S, Yoo JJ, Retik AB. Tissue-engineered autologous bladders for patients needing cystoplasty. Lancet 2006;367(9518):1241–6.
[46] Furth ME, Atala A, Van Dyke ME. Smart biomaterials design for tissue engineering and regenerative medicine. Biomaterials 2007;28(34):5068–73.
[47] Place ES, Evans ND, Stevens MM. Complexity in biomaterials for tissue engineering. Nat Mater 2009;8(6):457–70.
[48] Kao CT, Lin CC, Chen YW, Yeh CH, Fang HY, Shie MY. Poly(dopamine) coating of 3D printed poly(lactic acid) scaffolds for bone tissue engineering. Mater Sci Eng C Mater Biol Appl 2015;56:165–73.
[49] Haaparanta AM, Järvinen E, Cengiz IF, Ellä V, Kokkonen HT, Kiviranta I, et al. Preparation and characterization of collagen/PLA, chitosan/PLA, and collagen/chitosan/PLA hybrid scaffolds for cartilage tissue engineering. J Mater Sci Mater Med 2014;25(4):1129–36.
[50] Campbell JJ, Husmann A, Hume RD, Watson CJ, Cameron RE. Development of three-dimensional collagen scaffolds with controlled architecture for cell migration studies using breast cancer cell lines. Biomaterials 2017;114:34–43.
[51] Rossi E, Gerges I, Tocchio A, Tamplenizza M, Aprile P, Recordati C, et al. Biologically and mechanically driven design of an RGD-mimetic macroporous foam for adipose tissue engineering applications. Biomaterials 2016;104:65–77.
[52] Akbarzadeh R, Yousefi AM. Effects of processing parameters in thermally induced phase separation technique on porous architecture of scaffolds for bone tissue engineering. J Biomed Mater Res B Appl Biomater 2014;102(6):1304–15.
[53] Guarino V, Ambrosio L. The synergic effect of polylactide fiber and calcium phosphate particle reinforcement in poly epsilon-caprolactone-based composite scaffolds. Acta Biomater 2008;4(6):1778–87.
[54] Ghasemi-Mobarakeh L, Prabhakaran MP, Morshed M, Nasr-Esfahani MH, Ramakrishna S. Electrospun poly(epsilon-caprolactone)/gelatin nanofibrous scaffolds for nerve tissue engineering. Biomaterials 2008;29(34):4532–9.
[55] Orr SB, Chainani A, Hippensteel KJ, Kishan A, Gilchrist C, Garrigues NW, et al. Aligned multilayered electrospun scaffolds for rotator cuff tendon tissue engineering. Acta Biomater 2015;24:117–26.
[56] Hribar KC, Soman P, Warner J, Chung P, Chen S. Light-assisted direct-write of 3D functional biomaterials. Lab Chip 2014;14(2):268–75.
[57] Raya-Rivera A, Esquiliano DR, Yoo JJ, Lopez-Bayghen E, Soker S, Atala A. Tissue-engineered autologous urethras for patients who need reconstruction: An observational study. Lancet 2011;377(9772):1175–82.
[58] Warnke PH, Springer IN, Wiltfang J, Acil Y, Eufinger H, Wehmöller M, et al. Growth and transplantation of a custom vascularised bone graft in a man. Lancet 2004;364(9436):766–70.
[59] Bertassoni LE, Cardoso JC, Manoharan V, Cristino AL, Bhise NS, Araujo WA, et al. Direct-write bioprinting of cell-laden methacrylated gelatin hydrogels. Biofabrication 2014;6(2):024105.
[60] Cheng YL, Chen YW, Wang K, Shie MY. Enhanced adhesion and differentiation of human mesenchymal stem cell inside apatite-mineralized/poly(dopamine)-coated poly(ε-caprolactone) scaffolds by stereolithography. J Mater Chem B 2016;4(38):6307–15.
[61] Yeo M, Lee JS, Chun W, Kim GH. An innovative collagen-based cell-printing method for obtaining human adipose stem cell-laden structures consisting of core-sheath structures for tissue engineering. Biomacromolecules 2016;17(4):1365–75.
[62] Ouyang L, Highley CB, Sun W, Burdick JA. A generalizable strategy for the 3D bioprinting of hydrogels from nonviscous photo-crosslinkable inks. Adv Mater 2017;29(8):1604983.
[63] Guillemot F, Souquet A, Catros S, Guillotin B, Lopez J, Faucon M, et al. High-throughput laser printing of cells and biomaterials for tissue engineering. Acta Biomater 2010;6(7):2494–500.
[64] Guillemot F, Souquet A, Catros S, Guillotin B. Laser-assisted cell printing: Principle, physical parameters versus cell fate and perspectives in tissue engineering. Nanomedicine (Lond) 2010;5(3):507–15.
[65] Guillotin B, Souquet A, Catros S, Duocastella M, Pippenger B, Bellance S, et al. Laser assisted bioprinting of engineered tissue with high cell density and microscale organization. Biomaterials 2010;31(28):7250–6.
[66] Michael S, Sorg H, Peck CT, Koch L, Deiwick A, Chichkov B, et al. Tissue engineered skin substitutes created by laser-assisted bioprinting form skin-like structures in the dorsal skin fold chamber in mice. PLoS One 2013;8(3):e57741.
[67] Xu T, Zhao W, Zhu JM, Albanna MZ, Yoo JJ, Atala A. Complex heterogeneous tissue constructs containing multiple cell types prepared by inkjet printing technology. Biomaterials 2013;34(1):130–9.
[68] Yamazoe H, Tanabe T. Cell micropatterning on an albumin-based substrate using an inkjet printing technique. J Biomed Mater Res A 2009;91(4):1202–9.
[69] Tao H, Marelli B, Yang M, An B, Onses MS, Rogers JA, et al. Inkjet printing of regenerated silk fibroin: From printable forms to printable functions. Adv Mater 2015;27(29):4273–9.
[70] Tse C, Whiteley R, Yu T, Stringer J, MacNeil S, Haycock JW, et al. Inkjet printing Schwann cells and neuronal analogue NG108-15 cells. Biofabrication 2016;8(1):015017.
[71] Wüst S, Müller R, Hofmann S. Controlled positioning of cells in biomaterials—Approaches towards 3D tissue printing. J Funct Biomater 2011;2(3):119–54.
[72] Liu W, Zhang YS, Heinrich MA, De Ferrari F, Jang HL, Bakht SM, et al. Rapid continuous multimaterial extrusion bioprinting. Adv Mater 2017;29(3):1604630.
[73] Melchels FPW, Dhert WJA, Hutmacher DW, Mald J. Development and characterisation of a new bioink for additive tissue manufacturing. J Mater Chem B 2014;2(16):2282–9.
[74] Akkineni AR, Ahlfeld T, Lode A, Gelinsky M. A versatile method for combining different biopolymers in a core/shell fashion by 3D plotting to achieve mechanically robust constructs. Biofabrication 2016;8(4):045001.
[75] Ho CM, Mishra A, Lin PT, Ng SH, Yeong WY, Kim YJ, et al. 3D printed polycaprolactone carbon nanotube composite scaffolds for cardiac tissue engineering. Macromol Biosci 2017;17(4):1600250.
[76] Mironov V, Visconti RP, Kasyanov V, Forgacs G, Drake CJ, Markwald RR. Organ printing: Tissue spheroids as building blocks. Biomaterials 2009;30(12):2164–74.
[77] Itoh M, Nakayama K, Noguchi R, Kamohara K, Furukawa K, Uchihashi K, et al. Scaffold-free tubular tissues created by a Bio-3D printer undergo remodeling and endothelialization when implanted in rat aortae. PLoS One 2015;10(9):e0136681.
[78] Kolesky DB, Truby RL, Gladman AS, Busbee TA, Homan KA, Lewis JA. 3D bioprinting of vascularized, heterogeneous cell-laden tissue constructs. Adv Mater 2014;26(19):3124–30.
[79] Dávila JL, Freitas MS, Inforçatti Neto P, Silveira ZC, Silva JVL, d'Ávila MA. Fabrication of PCL/β-TCP scaffolds by 3D mini-screw extrusion printing. J Appl Polym Sci 2016;133(15):43031.
[80] Yeo M, Jung WK, Kim G. Fabrication, characterisation and biological activity of phlorotannin-conjugated PCL/β-TCP composite scaffolds for bone tissue regeneration. J Mater Chem 2012;22(8):3568–77.
[81] Montjovent MO, Mark S, Mathieu L, Scaletta C, Scherberich A, Delabarde C, et al. Human fetal bone cells associated with ceramic reinforced PLA scaffolds for tissue engineering. Bone 2008;42(3):554–64.
[82] Yu D, Li Q, Mu X, Chang T, Xiong Z. Bone regeneration of critical calvarial defect in goat model by PLGA/TCP/rhBMP-2 scaffolds prepared by low-temperature rapid-prototyping technology. Int J Oral Maxillofac Surg 2008;37(10):929–34.
[83] Roh HS, Lee CM, Hwang YH, Kook MS, Yang SW, Lee D, et al. Addition of MgO nanoparticles and plasma surface treatment of three-dimensional printed polycaprolactone/hydroxyapatite scaffolds for improving bone regeneration. Mater Sci Eng C 2017;74:525–35.
[84] Park SA, Lee SH, Kim WD. Fabrication of porous polycaprolactone/hydroxyapatite (PCL/HA) blend scaffolds using a 3D plotting system for bone tissue engineering. Bioprocess Biosyst Eng 2011;34(4):505–13.
[85] Gonçalves EM, Oliveira FJ, Silva RF, Neto MA, Fernandes MH, Amaral M, et al. Three-dimensional printed PCL-hydroxyapatite scaffolds filled with CNTs for bone cell growth stimulation. J Biomed Mater Res B Appl Biomater 2016;104(6):1210–9.
[86] Hortigüela MJ, Gutiérrez MC, Aranaz I, Jobbágy M, Abarrategi A, Moreno-Vicente C, et al. Urea assisted hydroxyapatite mineralization on MWCNT/CHI scaffolds. J Mater Chem 2008;18(48):5933–40.
[87] Wiria FE, Leong KF, Chua CK, Liu Y. Poly-ε-caprolactone/hydroxyapatite for tissue engineering scaffold fabrication via selective laser sintering. Acta Biomater 2007;3(1):1–12.
[88] Xia Y, Zhou P, Cheng X, Xie Y, Liang C, Li C, et al. Selective laser sintering fabrication of nano-hydroxyapatite/poly-ε-caprolactone scaffolds for bone tissue engineering applications. Int J Nanomedicine 2013;8:4197–213.
[89] Meng J, Xiao B, Zhang Y, Liu J, Xue H, Lei J, et al. Super-paramagnetic responsive nanofibrous scaffolds under static magnetic field enhance osteogenesis for bone repair *in vivo*. Sci Rep 2013;3:2655.
[90] Shor L, Güçeri S, Wen X, Gandhi M, Sun W. Fabrication of three-dimensional polycaprolactone/hydroxyapatite tissue scaffolds and osteoblast-scaffold interactions *in vitro*. Biomaterials 2007;28(35):5291–7.
[91] Xiao X, Liu R, Huang Q, Ding X. Preparation and characterization of hydroxyapatite/polycaprolactone-chitosan composites. J Mater Sci Mater Med 2009;20(12):2375–83.
[92] Endres M, Hutmacher DW, Salgado AJ, Kaps C, Ringe J, Reis RL, et al. Osteogenic induction of human bone marrow-derived mesenchymal progenitor cells in novel synthetic polymer-hydrogel matrices. Tissue Eng 2003;9(4):689–702.
[93] Rizzi SC, Heath DJ, Coombes AG, Bock N, Textor M, Downes S. Biodegradable polymer/hydroxyapatite composites: Surface analysis and initial attachment of human osteoblasts. J Biomed Mater Res 2001;55(4):475–86.
[94] Zhang H, Mao X, Du Z, Jiang W, Han X, Zhao D, et al. Three dimensional printed macroporous polylactic acid/hydroxyapatite composite scaffolds for promoting bone formation in a critical-size rat calvarial defect model. Sci Technol Adv Mater 2016;17(1):136–48.
[95] Senatov FS, Niaza KV, Stepashkin AA, Kaloshkin SD. Low-cycle fatigue behavior of 3D-printed PLA-based porous scaffolds. Composites, Part B 2016;97:193–200.
[96] Russias J, Saiz E, Nalla RK, Gryn K, Ritchie RO, Tomsia AP. Fabrication and mechanical properties of PLA/HA composites: A study of *in vitro* degradation. Mater Sci Eng C Biomim Supramol Syst 2006;26(8):1289–95.
[97] Senatov FS, Niaza KV, Zadorozhnyy MY, Maksimkin AV, Kaloshkin SD, Estrin YZ. Mechanical properties and shape memory effect of 3D-printed PLA-based porous scaffolds. J Mech Behav Biomed Mater 2016;57:139–48.
[98] Kutikov AB, Gurijala A, Song J. Rapid prototyping amphiphilic polymer/hydroxyapatite composite scaffolds with hydration-induced self-fixation behavior. Tissue Eng Part C Methods 2015;21(3):229–41.
[99] Kutikov AB, Song J. An amphiphilic degradable polymer/hydroxyapatite composite with enhanced handling characteristics promotes osteogenic gene

expression in bone marrow stromal cells. Acta Biomater 2013;9(9):8354–64.
[100] Zheng X, Zhou S, Li X, Weng J. Shape memory properties of poly(*D,L*-lactide)/hydroxyapatite composites. Biomaterials 2006;27(24):4288–95.
[101] Poh PSP, Hutmacher DW, Holzapfel BM, Solanki AK, Stevens MM, Woodruff MA. *In vitro* and *in vivo* bone formation potential of surface calcium phosphate-coated polycaprolactone and polycaprolactone/bioactive glass composite scaffolds. Acta Biomater 2016;30:319–33.
[102] Yao J, Radin S, S Leboy P, Ducheyne P. The effect of bioactive glass content on synthesis and bioactivity of composite poly (lactic-*co*-glycolic acid)/bioactive glass substrate for tissue engineering. Biomaterials 2005;26(14):1935–43.
[103] Serra T, Planell JA, Navarro M. High-resolution PLA-based composite scaffolds via 3-D printing technology. Acta Biomater 2013;9(3):5521–30.
[104] Kim Y, Kim G. Collagen/alginate scaffolds comprising core (PCL)–shell (collagen/alginate) struts for hard tissue regeneration: Fabrication, characterisation, and cellular activities. J Mater Chem B 2013;1(25):3185–94.
[105] Tsai KY, Lin HY, Chen YW, Lin CY, Hsu TT, Kao CT. Laser sintered magnesium-calcium pilicate/poly-ε-caprolactone scaffold for bone tissue engineering. Materials (Basel) 2017;10(1):65.
[106] Schantz JT, Brandwood A, Hutmacher DW, Khor HL, Bittner K. Osteogenic differentiation of mesenchymal progenitor cells in computer designed fibrin-polymer-ceramic scaffolds manufactured by fused deposition modeling. J Mater Sci Mater Med 2005;16(9):807–19.
[107] Charles-Harris M, Koch MA, Navarro M, Lacroix D, Engel E, Planell JAA. A PLA/calcium phosphate degradable composite material for bone tissue engineering: An *in vitro* study. J Mater Sci Mater Med 2008;19(4):1503–13.
[108] Wong HM, Chu PK, Leung FKL, Cheung KMC, Luk KDK, Yeung KWK. Engineered polycaprolactone—Magnesium hybrid biodegradable porous scaffold for bone tissue engineering. Prog Nat Sci Mater Int 2014;24(5):561–7.
[109] Kim YB, Kim GH. PCL/alginate composite scaffolds for hard tissue engineering: Fabrication, characterization, and cellular activities. ACS Comb Sci 2015;17(2):87–99.
[110] Lee H, Ahn S, Bonassar LJ, Kim G. Cell(MC3T3-E1)-printed poly(ε-caprolactone)/alginate hybrid scaffolds for tissue regeneration. Macromol Rapid Commun 2013;34(2):142–9.
[111] Zhang J, Zhao S, Zhu M, Zhu Y, Zhang Y, Liu Z, et al. 3D-printed magnetic Fe_3O_4/MBG/PCL composite scaffolds with multifunctionality of bone regeneration, local anticancer drug delivery and hyperthermia. J Mater Chem B 2014;2(43):7583–95.
[112] Nitya G, Nair GT, Mony U, Chennazhi KP, Nair SV. *In vitro* evaluation of electrospun PCL/nanoclay composite scaffold for bone tissue engineering. J Mater Sci Mater Med 2012;23(7):1749–61.
[113] Jin G, Kim G. The effect of sinusoidal AC electric stimulation of 3D PCL/CNT and PCL/β-TCP based bio-composites on cellular activities for bone tissue regeneration. J Mater Chem B 2013;1(10):1439–52.
[114] Mackle JN, Blond DJP, Mooney E, McDonnell C, Blau WJ, Shaw G, et al. *In vitro* characterization of an electroactive carbon-nanotube-based nanofiber scaffold for tissue engineering. Macromol Biosci 2011;11(9):1272–82.
[115] Saeed K, Park SY, Lee HJ, Baek JB, Huh WS. Preparation of electrospun nanofibers of carbon nanotube/polycaprolactone nanocomposite. Polymer 2006;47(23):8019–25.
[116] Anaraki NA, Rad LR, Irani M, Haririan I. Fabrication of PLA/PEG/MWCNT electrospun nanofibrous scaffolds for anticancer drug delivery. J Appl Polym Sci 2015;132(3):41286.
[117] Yang C, Chen S, Wang J, Zhu T, Xu G, Chen Z, et al. A facile electrospinning method to fabricate polylactide/graphene/MWCNTs nanofiber membrane for tissues scaffold. Appl Surf Sci 2016;362:163–8.
[118] Supronowicz PR, Ajayan PM, Ullmann KR, Arulanandam BP, Metzger DW, Bizios R. Novel current-conducting composite substrates for exposing osteoblasts to alternating current stimulation. J Biomed Mater Res 2002;59(3):499–506.
[119] Lee JS, Jin GH, Yeo MG, Jang CH, Lee H, Kim GH. Fabrication of electrospun biocomposites comprising polycaprolactone/fucoidan for tissue regeneration. Carbohydr Polym 2012;90(1):181–8.
[120] Luo Y, Wu C, Lode A, Gelinsky M. Hierarchical mesoporous bioactive glass/alginate composite scaffolds fabricated by three-dimensional plotting for bone tissue engineering. Biofabrication 2013;5(1):015005.
[121] Luo Y, Lode A, Sonntag F, Nies B, Gelinsky M. Well-ordered biphasic calcium phosphate-alginate scaffolds fabricated by multi-channel 3D plotting under mild conditions. J Mater Chem B 2013;1(33):4088–98.
[122] Wang K, Chang YH, Wang B, Zhang C. Printed electronics: Principles, materials, processes, and applications. In: Geng H, editor Semiconductor manufacturing handbook. 2nd ed. New York: McGraw-Hill Education; 2017. p. 245–316.